Intracellular Calcium Levels Correlate with Speed and Persistent Forward Motion in Migrating Neutrophils

John T. H. Mandeville, Richik N. Ghosh, and Frederick R. Maxfield
Departments of Pathology and Physiology, College of Physicians and Surgeons, Columbia University, New York 10032 USA

ABSTRACT The relationship between cytosolic free calcium concentration ($[Ca^{2+}]_i$) and human neutrophil motility was studied by video microscopy. Neutrophils stimulated by a uniform concentration of an *N*-formylated peptide chemoattractant (f-Met-Leu-Phe) were tracked during chemokinetic migration on albumin, fibronectin, and vitronectin. $[Ca^{2+}]_i$ buffering with quin2 resulted in significant decreases in mean speed on albumin. To further characterize the relationship between $[Ca^{2+}]_i$ changes and motility we carried out a cross-correlation analysis of $[Ca^{2+}]_i$ with several motility parameters. Cross-correlations between $[Ca^{2+}]_i$ and each cell's speed, angle changes, turn strength, and persistent forward motion revealed (i) a positive correlation between $[Ca^{2+}]_i$ and cell speed ($p < 0.05$), (ii) no significant correlation between turns and calcium spikes, and (iii) the occurrence of turns during periods of low speed. Significant negative correlations between $[Ca^{2+}]_i$ and angle change were noted on the high adhesion substrates vitronectin and fibronectin but not on the low adhesion substrate albumin. These data imply that there is a general temporal relationship between $[Ca^{2+}]_i$, speed, and persistent motion. However, the correlations are not sufficiently strong to imply that changes in $[Ca^{2+}]_i$ are required proximal signals for velocity changes.

INTRODUCTION

Neutrophils, or polymorphonuclear leukocytes, can rapidly migrate through the extracellular matrix toward a chemoattractant source, such as a site of bacterial infection (Cassimeris and Zigmond, 1990; Devreotes and Zigmond, 1988). This directed cell migration is crucial for defense against microbes, and it also plays an important role in inflammation. In the presence of an isotropic gradient of chemoattractant, neutrophils exhibit nondirected motion, known as chemokinesis (Gruler and Bultmann, 1984; Hall and Peterson, 1979; Zigmond and Hirsch, 1973). Cells proceed through velocity cycles, including periods when they pause and reorient themselves. In an anisotropic gradient of chemoattractant, neutrophils exhibit directed motion, known as chemotaxis, which resembles chemokinesis except that turns in the direction of the chemoattractant source are favored (Caterina and Devreotes, 1991; Devreotes and Zigmond, 1988).

Cell locomotion requires a complex series of steps, which include attachment to the substrate, generation of force, and detachment from the substrate (Lee et al., 1993). These processes must be regulated in a coordinated manner to result in productive motion. Adhesion to the substrate is mediated by cell surface receptors, such as integrins (Hynes, 1992). Integrins are heterodimeric molecules capable of both generating and responding to intracellular signals that can modulate their substrate affinity (Schwartz, 1992). Propulsive force can be generated by (i) molecular motors such as the myosin family, (ii) polymerization of cytoskeletal subunits, probably actin, and (iii) osmotic pressure derived by gel to sol transition of the cytoskeleton. Myosin II molecules have been localized to the rear of polarized cells and could generate contractile force to squeeze the cytoplasm forward (Eliott et al., 1993; Wessels and Soll, 1990), whereas myosin I molecules have been localized to the front of polarized cells and have been implicated in cortical expansion and pseudopod retraction (Fukui et al., 1989; Wessels et al., 1991). The cortical expansion model predicts that the major protrusive forces are generated by the polymerization of actin filaments in the leading edge (Condeelis et al., 1990), whereas the nucleation-release model argues that actin treadmilling is harnessed to drive extension by anchoring of filaments at adhesion points by some kind of slippable molecular clutch (Theriot and Mitchison, 1991). Osmotic pressure could be generated by solation of the actin network, weakening the elastic modulus and creating osmotically active actin fragments (Sheterline and Rickard, 1989).

Cytosolic free calcium levels ($[Ca^{2+}]_i$) could affect many stages of the motility process (see Maxfield, 1993, for recent review). Indirect effects could be mediated by kinases such as protein kinase C and myosin light chain kinase, which are calcium dependent. Direct effects could include fragmentation and nucleation of the actin cytoskeleton via calcium-regulated molecules such as gelsolin (Cunningham et al., 1991), MARCKS (Hartwig et al., 1992), and fodrin (Harris and Morrow, 1990). Increases in $[Ca^{2+}]_i$ can also lead to decreased affinity of certain integrins for their extracellular ligands (Hendey et al., 1992).

Migrating neutrophils stimulated by the bacterially derived chemoattractant f-Met-Leu-Phe (fMLP) exhibit transient increases in $[Ca^{2+}]_i$ from a relatively steady baseline that vary in magnitude, timing, and duration (Jaconi et al., 1991; Marks and Maxfield, 1990b). When these $[Ca^{2+}]_i$ transients are buffered with quin2 or BAPTA, locomotion is inhibited on specific substrates, although the cells are still able

Received for publication 2 June 1994 and in final form 6 January 1995.
Address reprint requests to Dr. Frederick R. Maxfield, Department of Pathology, College of Physicians and Surgeons, Columbia University, 630 W. 168th St., New York, NY 10032. Tel.: 212-305-4090; Fax: 212-305-5498; E-mail: fred@curadt.path.columbia.edu.

0006-3495/95/04/1207/11 $2.00

to change their morphology and generate pseudopods (Marks and Maxfield, 1990b). This inhibition was shown to be specific to neutrophils migrating on vitronectin and fibronectin, components of the extracellular matrix, whereas neutrophils on albumin can still migrate but with decreased speed (Marks et al., 1991). $[Ca^{2+}]_i$ transients seem to be required for decreasing the affinity of an integrin for vitronectin, mediated by a dephosphorylation event, thereby allowing the cells to move forward (Hendey et al., 1992).

In human neutrophils, imaging experiments with fura-2 did not reveal persistent intracellular $[Ca^{2+}]_i$ gradients during chemotaxis or chemokinesis that might account for the direction of cell movement (Marks and Maxfield, 1990a). However, $[Ca^{2+}]_i$ gradients on the order of 1 nM/μm, increasing from front to rear, have been reported in other cell types, such as *Amoeba proteus* (Gollnick et al., 1991), newt eosinophils (Brundage et al., 1991, 1993), and fish keratocytes (Brust-Mascher et al., 1994). As neutrophils, averaging $\sim$10 μm in diameter, are many times smaller than these cell types, it is possible that such minute gradients were not detectable. The transient increases in $[Ca^{2+}]_i$ throughout the cell, on the order of hundreds of nanomolar, would be much larger than these small gradients even if they do exist. Brundage et al. (1991, 1993) also reported the presence of transient elevations in $[Ca^{2+}]_i$ that accompanied turns in migrating eosinophils. However, these data were collected from relatively few cells.

It has been observed that migrating neutrophils undergo a three-dimensional motility cycle, during which they periodically pause and raise their leading edge off the substratum before re-contacting the surface and changing direction (Murray et al., 1992). This behavior would be consistent with decreased attachment to the substrate and reorganization of the cytoskeleton before increasing speed in a new direction. Each of these steps could be affected by changes in $[Ca^{2+}]_i$, as described above.

We speculated that $[Ca^{2+}]_i$ transients could lead to quantifiable changes in cell motion such as speed and direction changes, and that the temporal relationship between $[Ca^{2+}]_i$ and changes in motility parameters might provide insights into the role that $[Ca^{2+}]_i$ was playing. Using measurements from a large number of cells, we attempted to determine whether a correlation existed between $[Ca^{2+}]_i$ and turns or between $[Ca^{2+}]_i$ and speed changes in migrating human neutrophils.

Cross-correlation analyses between total cell $[Ca^{2+}]_i$ and motility parameters were performed for cells migrating on albumin, fibronectin, and vitronectin. We found that a statistically significant positive correlation exists between relative calcium levels and cell speed. Calcium transients tended to precede, but did not appear to be required for, increases in speed. In addition, we found a significant positive correlation between $[Ca^{2+}]_i$ and persistent forward motion, and no correlation between $[Ca^{2+}]_i$ and turns. These correlations were not substrate specific with the exception of angle change, for which a significant negative correlation with $[Ca^{2+}]_i$ was seen only on the high adhesion substrates vitronectin and fibronectin. These data imply a general timing relationship between $[Ca^{2+}]_i$ and speed or persistent motion, but they do not imply that changes in $[Ca^{2+}]_i$ are required proximal signals for changes in speed or direction.

MATERIALS AND METHODS

Isolation of neutrophils

Human whole blood was obtained by syringe from apparently healthy volunteers and immediately placed in polypropylene tubes containing sodium heparin (Becton Dickinson, San Jose, CA). Neutrophils were isolated by centrifugation for 30 min at 400 *g* over a Ficoll-Hypaque solution (1-Step Polymorphs, Accurate Chemical and Scientific, Westbury, NY). Contaminating erythrocytes were removed by a 30-s hypotonic lysis procedure. Cells were then rinsed in phosphate-buffered saline (137 mM NaCl, 2.7 mM KCl, 8.1 mM Na_2HPO_4, 1.5 mM KH_2PO_4, pH 7.4) and resuspended in incubation media (150 mM NaCl, 5 mM KCl, 1 mM $MgCl_2$, 1 mM $CaCl_2$, 20 mM HEPES, 10 mM glucose, pH 7.4). Preparations contained >95% neutrophils, as assessed by their characteristic morphology.

Loading with calcium indicators and buffers

Neutrophils were loaded as previously described (Marks et al., 1991). Briefly, cells were tumbled for 40 min at room temperature in loading buffer (2% heat-inactivated calf serum, incubation buffer with 0.2% dimethylsulfoxide, and 0.02% w/v pluronic F-127; Molecular Probes, Eugene, OR) containing the cell-permeable acetoxymethyl ester (AM) forms of the dyes as indicated below. Cells were then rinsed in phosphate-buffered saline, resuspended in incubation media, and stored over ice until use. For calcium imaging experiments, neutrophils were treated as above in loading buffer containing 5 μM fura-2/AM (Molecular Probes). For calcium measurement and tracking experiments, neutrophils were loaded in 10 μM fluo-3/AM (Molecular Probes). In calcium-buffering experiments, cells were loaded with 50 μM quin2/AM (Molecular Probes). Cells were always used within 5 h of loading.

Two procedures were used to verify the cytoplasmic loading of fluo-3/AM under the conditions used, as compartmentalization of AM-loaded dyes has been previously reported (Scanlon et al., 1987). Optimization of the fura-2/AM loading procedure has been described in detail (Marks and Maxfield, 1990a). First, neutrophils loaded with fluo-3/AM as described above were ruptured in a Dounce homogenizer in 0.2 M sucrose, 20 mM EDTA, 20 mM HEPES, pH 7.0, on ice (Ratan et al., 1986). The homogenate was then centrifuged at 10,000 *g* for 1 min to remove nuclei and unruptured cells. The post-nuclear supernatant was layered over a 0.4 M sucrose cushion and centrifuged at 100,000 *g* for 15 min at 4°C. The supernatant and pellet were separated and examined for calcium-sensitive fluo-3 fluorescence on an SLM 8000C spectrofluorometer (SLM Instruments, Urbana, IL) after addition of 0.1% Triton X-100 (Sigma Chemical Co., St. Louis, MO) to the fractions to release the contents of membrane-bound organelles. We found >97% of fluo-3 fluorescence in the supernatant (n = 2), indicating that nearly all of the dye was in the cytosol.

The second procedure we used was selective permeabilization of the plasma membrane by digitonin (Poenie et al., 1987). Fluo-3-loaded neutrophils were observed by video fluorescence microscopy as increasing doses of digitonin (Sigma) were added to the media. The cells were permeabilized at $\sim$20 μM digitonin, a concentration known to release cytoplasmic contents while leaving intracellular organelles intact (Yamashiro et al., 1983). Using the quantitative methods described below, cell fluorescence a few seconds before and after permeabilization were compared. We found an average of 92% of fluo-3 fluorescence could be released with digitonin (n = 171). Taken together, we conclude that <10% of fluo-3 is in intracellular organelles.

Microscope system

Simultaneous fluorescence and Nomarski differential interference contrast (DIC) images of migrating cells were acquired using a Leitz-Diavert

microscope (Wetzlar, Germany) that was modified according to the method of Foskett (1988). As the emission wavelengths of our dyes do not exceed 600 nm, it is possible to use red light (>620 nm) for DIC imaging without interfering with the fluorescence signal. Samples were illuminated at both DIC and fluorescence excitation wavelengths. Light from a 100-W Xenophot lamp (Osram GmbH, Munich, Germany) was passed through a 640-nm bandpass filter (40-nm bandwidth, DF series, Omega Optics, Brattleboro, VT) for DIC imaging. Illumination of the samples at appropriate excitation wavelengths was as previously described (Marks et al., 1988).

Light coming from the sample was separated by a 580-nm dichroic beamsplitting mirror mounted at 45° relative to the optical axis of the microscope. Fluorescence emission light was reflected by the mirror through a 507-nm bandpass filter (42-nm bandwidth, DF series, Omega Optics) to an image intensifier (Model KS-1381, Videoscope International, Washington, DC) and collected by a charge-coupled device (CCD) video camera (CCD-72, MTI-Dage, Michigan City, IN). DIC light was passed by the mirror through a 620-nm longpass filter (Ditric Optics, Hudson, MA) and analyzer and collected by a CCD video camera (CCD-72, MTI-Dage) with the infrared filter removed. Final DIC and fluorescence images obtained were parfocal and mirror images of one another. To prevent crossover between the two light paths, high quality filters (<0.01% transmittance two bandwidths from center) were used.

Fura-2 imaging

Fura-2 imaging was performed as previously described (Marks and Maxfield, 1990a). Briefly, fura-2-loaded neutrophils were plated on coverslip bottom dishes coated with 1 mg/ml albumin (Sigma) purified as previously described (Marks et al., 1991). Coverslip bottom dishes were made using coverslips cleaned with Nochromix (Godax Labs, New York, NY) attached to the underside of tissue culture dishes with holes punched in the bottom, followed by adsorption of the substrate. Neutrophils were allowed to adhere at 37°C for 5 min in incubation media, followed by a 5-min stimulation with 10 nM fMLP (Sigma).

Fura-2 fluorescence was excited at 340 and 380 nm by rapidly switching between illumination sources (Marks et al., 1988). Cells were imaged with the microscope described above with a 100× Nikon UV Fluor objective (N.A. = 1.3). Simultaneous DIC and fluorescence images were recorded onto monochrome high resolution optical disk recorders (Model TQ-2028F, Panasonic, Secaucus, NJ) controlled by a personal computer. Image processing was performed using a Gould IP9000 image processor (Vicom, Fremont, CA) linked to a Micro Vax II (Digital Equipment, Maynard, MA) as the host computer. Four consecutive frames were digitized, averaged, and subjected to a 16 × 16 pixel Gaussian convolution filter, and background was corrected. The 340-nm images were divided by the previous and following 380-nm images and pseudocolored, yielding a temporal resolution of approximately 0.5 s and a reliable spatial resolution of roughly 4 μm^2 (Marks and Maxfield, 1990a).

The advantages of using fura-2 as a calcium indicator are that by taking the ratio of 340 to 380 nm fluorescence, one can avoid measurement artifacts due to cell thickness, dye concentration, and interference by competing ions, thus allowing excellent subcellular localization of $[Ca^{2+}]_i$. However, preliminary results presented here, as well as those described by Marks and Maxfield (1990), indicated that the $[Ca^{2+}]_i$ events of interest were global rather than local. This permitted us to switch to the highly sensitive nonratiometric calcium indicator fluo-3, thereby obviating the need for intensive image processing. The contribution of localized changes in $[Ca^{2+}]_i$ to the regulation of neutrophil motility remains to be examined in further detail.

Fluo-3 measurements and cell tracking

Motility assays were performed as previously described (Marks et al., 1991). Briefly, coverslip bottom dishes were coated with one of the following substrates: 1 mg/ml purified albumin, 0.1 mg/ml fibronectin (Telios Pharmaceuticals, San Diego, CA), or 0.01 mg/ml vitronectin (Telios Pharmaceuticals). Neutrophils were allowed to attach to the substrate at 37°C for 5 min in incubation media, followed by a 5-min stimulation with a bath application of 10 nM fMLP. Simultaneous fluorescence and DIC images of migrating cells were recorded with a single super-VHS videotape recorder (JVC, Elmwood Park, NJ) with the microscope assembly described above. Fluo-3 fluorescence was detected using fluorescein optics (490 excitation, 525 emission), a Nikon Fluor 40× objective (N.A. = 0.8), video intensifier, CCD camera, and frame averager (MTI-Dage). Experiments were performed on multiple substrates each day to account for variability among neutrophil batches.

Videotaped data were digitized at 5-s intervals for 240 to 300 s, using a DOS-based system (Image-1, Universal Imaging Corp., West Chester, PA). The coordinates of each cell centroid were determined manually from the DIC image and stored for further processing. The entire cell area, including lamellipodia, was considered in centroid determination. The precision in determining the centroid location manually was estimated to be <0.5 μm, as judged by reproducibility of the data in 30 repeat measurements by a single observer; the accuracy was judged to be 0.50 ± 0.04 μm (SE; $n = 30$) by comparison with the centroid defined by an outline of the cell traced from the DIC image, computed with public domain software (NIH Image, written by Wayne Resband, available to Internet users from zippy.nimh.nih.gov). Cells that did not move >7 μm in 300 s were discarded from analysis. Whole cell $[Ca^{2+}]_i$ was measured as mean fluo-3 fluorescence, calculated as the average pixel intensity of a region completely encompassing the cell, minus background fluorescence. To determine whether cell area affected the measurement of total cell fluorescence, cells were loaded with 10 μM of the calcium-insensitive dye calcein/AM (Molecular Probes) and imaged every 5 s during migration by using the same methods as for fluo-3/AM. During a 5-min observation period, the total cell fluorescence varied by 5% (SD; $n = 25$), and the mean cell area was 120 ± 21 μm^2. The whole cell fluorescence at each time point was normalized to the mean cell fluorescence over the 5-min observation period for that cell ($n = 60$) and plotted versus cell area. The best fit line was calculated by linear regression for each cell, and the average slope was calculated; this slope corresponded to a 2.5 ± 0.9% (SE) decrease in fluorescence per 100 μm^2 increase in area. We therefore conclude that changes in cell shape have a negligible effect on cell fluorescence. An example of raw data is given in Fig. 1, from which tracking and $[Ca^{2+}]_i$ measurements were made. Because of day-to-day variability in cell loading, lamp intensities, and image acquisition settings, the

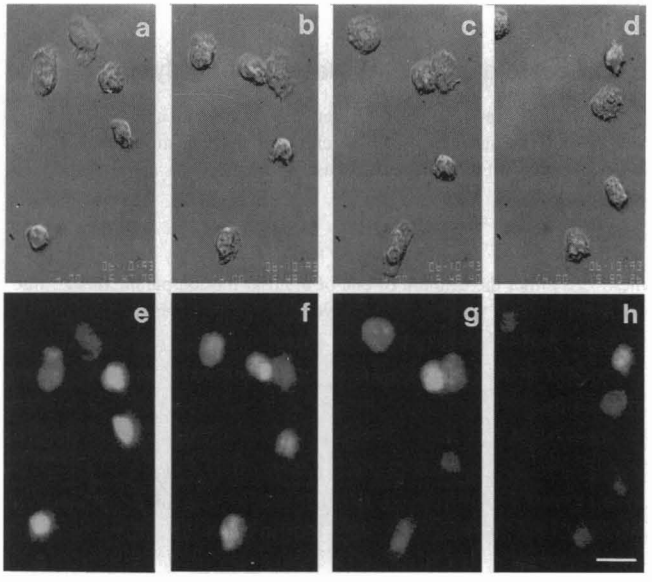

FIGURE 1 Simultaneous imaging of the position and $[Ca^{2+}]_i$ of migrating neutrophils by DIC and fluorescence microscopy. Cells were loaded with the Ca^{2+}-sensitive dye fluo-3. Panels were chosen to illustrate movement of cells during a 5-min recording period (*a-d*) as well as associated changes in fluorescence intensities (*e-h*). Whole cell Ca^{2+} was measured as the mean fluorescence pixel intensity within a region encompassing the cell. Time is indicated on the DIC panels. Bar, 20 μm.

calcium data were normalized as described in detail below (see Eq. 2). This normalization procedure enabled us to compare changes in $[Ca^{2+}]_i$ among separate experiments, but we did not obtain a measurement of absolute $[Ca^{2+}]_i$.

Motion parameters

We examined four motion parameters of the tracked cell at each time point i: speed, angle change, and the perpendicular and parallel projections of the outgoing vector on the incoming vector. The 5-s interval between frames was too fine a time resolution to detect large changes in the neutrophils' motion over the frame-to-frame fluctuations, so in our analysis we defined our motion parameters over a longer (20-s) time interval. (Although data analysis was performed using 10-, 20-, and 40-s time rulers with qualitatively similar results, all data presented here were derived using a 20-s time ruler. This time interval gave the best agreement with turns arbitrarily defined by multiple observers while reducing noise derived from small deviations in the cell path.) Fig. 2 illustrates how the motion parameters were defined. Each time point i is separated by 5 s, but the speed at time i, s_i, is defined as the magnitude of the vector going from the cell's position at time $i - 2$ to the position at $i + 2$, divided by the intervening time interval, 20 s. In other words, the speed is defined as the distance the cell travels in a 20-s interval, from its location 10 s before to 10 s after its current location, and this is computed for each time point i. Two vectors, **a** and **b**, are also defined at each time point i as shown in Fig. 2. Vector **a** is the incoming vector, which goes from the cell's position 20 s before i (i.e., $i - 4$), to the current position at i, and vector **b** is the outgoing vector, which goes from the current position to the position 20 s later. The angle change at i, θ_i, is defined as the absolute value in the angle change between vectors **a** and **b**. The perpendicular projection of the outgoing vector on the incoming vector measures the vector component in the direction of the turn and is defined as the product of the magnitude of **b** with the sine of θ_i. Similarly, the degree to which the cell continued traveling in the same direction and did not turn is defined as the parallel projection of the outgoing vector on the incoming vector and is computed as the product of the magnitude of **b** with the cosine of θ_i. We define these as the turn strength and the persistence, respectively. Although the four parameters we examine are all interrelated and ultimately derived from velocity vectors, they emphasize different aspects of cell motion.

Cross-correlations and statistical analysis

To determine the timing relationship between the calcium and mobility data, the cross-correlations between the calcium and the four motion parameters were determined. First, the mean was subtracted from each of the five parameters:

$$\mathbf{Y}_i = Y_i - \langle Y \rangle \tag{1}$$

where Y_i is either the calcium or one of the four motion parameters at time point i, and $\langle Y \rangle$ is the mean value over all the time points i. The mean-subtracted parameter $\mathbf{Y}_i$ was then normalized in the following manner, so that the sum of the area under the auto-correlation would be 1:

$$y_i = \frac{\mathbf{Y}_i}{\sqrt{\sum_{i=1}^{N} \mathbf{Y}_i^2}} \tag{2}$$

where there are N time points i, and the normalized mean-subtracted parameter is y_i. The cross-correlations, x_j, between the normalized mean-subtracted calcium, c, and each of the four normalized mean-subtracted motion parameters, y, were computed for various lag times j:

$$x_j = (y * c)_j \tag{3}$$

The cross-correlation between y and c (denoted by $*$) was computed by multiplying the Fourier transform of y with the complex conjugate of the Fourier transform of c and then computing the inverse transform of the product, using the algorithms of Press et al. (1986). The convention used is that if a peak in speed occurred j seconds after a calcium peak, a positive cross-correlation would be seen at a positive lag time of j seconds (i.e., the speed lags the calcium by j seconds).

This cross-correlation analysis was done between calcium and the four motion parameters for all the cells. The mean cross-correlation $\langle x_j \rangle$ at each lag time j over all M cells was also determined, for each of the four motion parameters:

$$\langle x_j \rangle = \frac{1}{M} \sum_{k=1}^{M} x_{j,k} \tag{4}$$

where $x_{j,k}$ is the cross-correlation at lag j for cell k. We also determined how significantly different from zero the mean cross-correlation was at each lag j, by doing an unpaired Student's t-test on the distribution of cross-correlations from the M cells at each lag j. The t-test is valid for normally distributed data, and the cross-correlations at each lag time j were normally distributed, as ascertained by the skew and kurtosis for each of the distributions that were significant at the 95% confidence level (Sokal and Rohlf, 1981). Normality was also established by a Lilliefors test for normality with a 95% confidence level (Cembrowski et al., 1979; Lilliefors, 1967). To determine which of the mean cross-correlation peaks indicated to be significantly non-zero by the t-test were not occurring by chance, a Bonferroni test was done for each distribution (Glantz, 1992). The Bonferroni parameter is determined from the cutoff probability value for significance used in the t-test (0.05) divided by the total number of distributions looked at (20), giving a value of 0.0025. The means of the distributions that had a significance p value < 0.0025 were deemed unlikely to be occurring by chance. The Bonferroni test is considered overly conservative for greater than 10 distributions (Glantz, 1992) but was employed for its ease in use and to identify distribution means highly unlikely to be occurring by chance. As a control, the calcium and motion parameters from unmatched cells were cross-correlated, and the means of these distributions at the different lag times j were found not to be statistically different from zero ($p > 0.05$). An example of these control data is given for the cross-correlation of calcium with velocity (see Fig. 7 *E*); cross-correlations for other motility parameters were similar (data not shown).

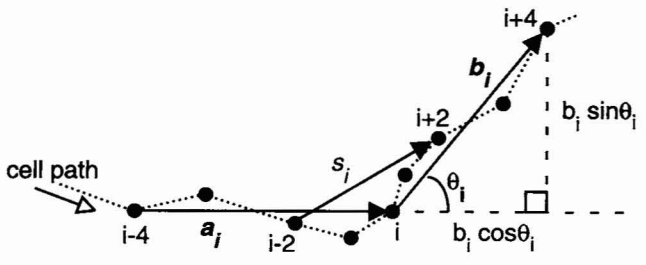

FIGURE 2 Definitions of motion parameters. Hypothetical track of a cell centroid with vectors illustrating definitions of speed ($|s_i|$), angle change (θ_i), persistence ($|b_i| \cos \theta_i$), and turn strength ($|b_i| \sin \theta_i$), for a cell at position i.

RESULTS

Calcium buffering alters speed

To examine the role of $[Ca^{2+}]_i$ transients in cell motility, we used 50 μM quin2/AM to dampen the $[Ca^{2+}]_i$ transients and lower basal $[Ca^{2+}]_i$ levels as previously described (Hendey et al., 1992; Marks and Maxfield, 1990b). As quin2-buffered cells are unable to migrate on fibronectin or vitronectin (Marks et al., 1991), these experiments were performed on the less adhesive substrate albumin. Cell centroids were tracked at 10-s intervals for 6 min during chemokinesis stimulated with fMLP. Representative fields from a tracking experiment of control and quin2-buffered cells are shown in

Fig. 3, *A* and *B*, respectively. The results of the motion analysis are summarized in Table 1.

Motion analysis revealed that movement on albumin is decreased, but not completely inhibited, by calcium buffering, confirming previous experiments (Marks et al., 1991). The net distance traveled, defined as the distance between the neutrophil's initial position and its final position 6 min later, when averaged over 120 control cells, was 19.9 ± 1.3 μm. Calcium-buffered neutrophils moved a mean net distance of 16.4 ± 0.8 μm (n = 128), which is 82% of the net distance of control cells. This difference is statistically significant at the $p < 0.02$ confidence level by the unpaired Student's t-test. Furthermore, the mean speed of the buffered cells (defined as the total distance traveled divided by the total observation time) was 4.97 ± 0.11 μm/min, which is 76% that of controls ($p \ll 0.001$), indicating that the suppression of $[Ca^{2+}]_i$ transients leads to a lower average cell speed.

Calcium-buffered cells also appeared to turn less than control cells. As the definition of a turn can be extremely arbitrary, we quantified turns using three definitions measuring different aspects of the turn: the angle change and the perpendicular and parallel projections of the outgoing vector, the latter two measuring the degree to which the cell either turned or persisted moving forward, respectively (defined as turn strength and persistence; see Materials and Methods). With a 20-s time ruler, control cells exhibited a mean angle change of 60°, similar to the finding of others (Hall and Peterson, 1979), whereas buffered cells exhibited a mean angle change of 56°. As neutrophils move in a stop-and-go fashion, large angle changes can result from small changes in centroid location during low speed searching behavior, during which the cell extends and retracts pseudopodia. To reduce the contribution of searching behavior to the measurement of turns, we used the turn strength and persistence, which contain both angle and speed information, as another means of examining turns. We found that quin2-buffered cells had a lowered turn strength (72% of controls, $p \ll 0.001$), yet also had a lowered persistence (79% of controls, $p < 0.001$). These apparently conflicting results probably reflect a general reduction in movement in quin2-buffered cells, as speed is a component of our definitions of both turn strength and persistence.

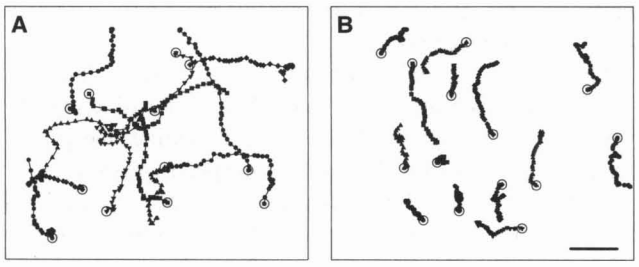

FIGURE 3 Trajectories of neutrophils migrating on albumin with or without $[Ca^{2+}]_i$ buffering by quin2. Symbols indicate the location of cell centroids at 10-s intervals from two representative fields; circled symbols indicate initial position. Cells were tracked for 6 min in the presence of a uniform concentration of fMLP. (*A*) Control cells. (*B*) Quin2-buffered cells. $[Ca^{2+}]_i$-buffered cells are able to migrate and turn on albumin but with decreased speed (see Table 1). Bar, 20 μm.

TABLE 1 Effects of calcium buffering on neutrophil motility over albumin-coated glass

Parameter	Control (n = 120)	Quin2 (n = 128)	p value*
Net displacement‡ (μm)	19.9 ± 1.26§	16.4 ± 0.78	0.0177
Speed‖ (μm/min)	6.51 ± 0.21	4.97 ± 0.11	≪0.0001
Angle change (deg)	59.8 ± 1.74	55.5 ± 1.75	0.0851
Turn strength (μm)	0.97 ± 0.03	0.70 ± 0.02	≪0.0001
Persistence (μm)	1.53 ± 0.07	1.21 ± 0.04	0.0001

*p values obtained by unpaired Student's t-test, null hypothesis being that control and calcium-buffered groups are the same.
‡Net distance traveled during 6-min observation period (difference between positions at first and last points).
§Values given as mean ± SE.
‖Total distance traveled divided by the total observation time.

Fura-2 imaging of global $[Ca^{2+}]_i$ changes during turns

To determine the role of $[Ca^{2+}]_i$ transients in changing the speed or direction of cell migration, we began by looking for intracellular $[Ca^{2+}]_i$ gradients during cell turning by using the ratiometric calcium indicator fura-2. Cells were simultaneously visualized by DIC microscopy. Preliminary results failed to demonstrate polarized subcellular elevations in $[Ca^{2+}]_i$ during neutrophil turning on albumin-coated glass. Fig. 4 illustrates a cell spontaneously changing direction in the presence of a uniform concentration of fMLP. The cell underwent a large global increase in $[Ca^{2+}]_i$ as it paused, rounded slightly, and then proceeded in a new direction. The $[Ca^{2+}]_i$ increase also seemed to be accompanied by intense ruffling of the cell membrane. The highly localized spots of inhomogeneity we observed have been previously described (Marks and Maxfield, 1990a) and are partially attributable to noise characteristics of the image acquisition system. In particular, noise is contributed by the high gains of the image intensifier, needed to detect the low 380-nm signal from thin regions of the cell, as well as by low temporal averaging, necessary to detect rapid changes in $[Ca^{2+}]_i$. The spots appear only transiently (<1 s) and are therefore unlikely to represent stable intracellular compartments. Rapid, highly localized increases in $[Ca^{2+}]_i$ may indeed play a role in cell motility, but this remains to be explored. As the $[Ca^{2+}]_i$ increased throughout the cell with no clear gradient, and previous experiments failed to demonstrate consistent calcium gradients within migrating neutrophils (Marks and Maxfield, 1990a), for additional $[Ca^{2+}]_i$ measurements we switched to the use of a sensitive nonratiometric calcium indicator fluo-3, which does not require intensive image processing.

Single cell analysis of $[Ca^{2+}]_i$ and motion

To study the relationship of global changes in $[Ca^{2+}]_i$ to turns and speed, a large number of fluo-3-loaded cells were tracked during fMLP-stimulated chemokinesis on three different

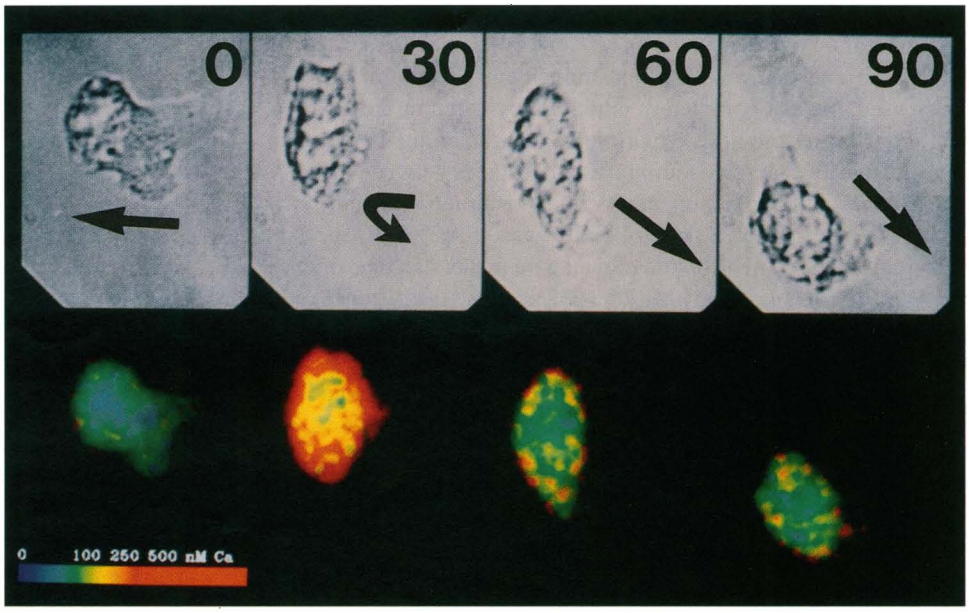

FIGURE 4 Simultaneous DIC and pseudocolored $[Ca^{2+}]_i$ images of a migrating neutrophil undergoing a change in direction in the presence of a uniform gradient of fMLP. Images are shown at 30-s intervals, as indicated. The fura-2-loaded cell was moving to the left (time 0), then paused and displayed a large, global increase in $[Ca^{2+}]_i$ that was associated with intense membrane ruffling (30 s). The cell then resumed motion to the lower right as $[Ca^{2+}]_i$ decreased, but remained above initial levels (60 and 90 s). Direction of motion is indicated by arrows. Calcium levels indicated by color bar. Bar, 25 μm.

substrates: albumin (n = 60), fibronectin (n = 61), and vitronectin (n = 73). Fig. 1 illustrates a typical tracking experiment. Total cell calcium levels (as fluo-3 fluorescence) and location of the cell centroid were determined at 5-s intervals for 4 to 5 min.

We examined the relationship between $[Ca^{2+}]_i$ transients and turns and observed a wide variety of behaviors, illustrated in Fig. 5. Some turns were accompanied by $[Ca^{2+}]_i$ spikes. These spikes could occur before, during, or after a turn, and several examples can be seen in Fig. 5 (e.g., cells *C-3* and *A-2*). However, cells could turn with no preceding $[Ca^{2+}]_i$ elevations for >60 s. Cells *D-3* and *C-2* in Fig. 5 demonstrate turns that are not accompanied by $[Ca^{2+}]_i$ transients. And finally, some cells (e.g., cell *B-3*) showed multiple $[Ca^{2+}]_i$ spikes during persistent forward movement. In addition to turning behavior, one can also note changes in speed from the cell trajectories in Fig. 5, speed being indicated by the spacing between symbols. Whereas cells *D-2* and *A-3* show increased speed during periods of high $[Ca^{2+}]_i$, cells *B-1* and *A-1* show high speed during periods of low $[Ca^{2+}]_i$.

The motility parameters and normalized $[Ca^{2+}]_i$ were determined for each cell, and examples are illustrated in Fig. 6. The calcium record has been normalized and the mean subtracted (see Materials and Methods). The speed was frequently seen to reach a peak concurrently with, or slightly following, a rise in $[Ca^{2+}]_i$ (Fig. 6 *A*, corresponding to cell *A-3* in Fig. 5). However, in some cases, speed peaks could occur with no associated calcium rise, or they could occur in advance of a calcium transient. As seen in Fig. 6 *A*, turns defined simply as the angle change tend to occur during periods of very low speed. However, by looking at the turn strength and persistence together, both of which incorporate a speed term in their definitions, we did not see a general relationship between turns and $[Ca^{2+}]_i$. By comparing the motility data in Fig. 6 *B* with the corresponding cell trajectory in Fig. 5 (cell *C-1*), one can easily see instances for which turn strength corresponds to changes in direction. To determine whether any statistically significant temporal relation existed between $[Ca^{2+}]_i$ and the cells' motility parameters, we computed the cross-correlation of each cell's $[Ca^{2+}]_i$ and the four motility parameters and then averaged the results.

Speed correlates with changes in $[Ca^{2+}]_i$

The convention used in our cross-correlation analysis results in a positive correlation if the motility parameter associates positively with the behavior of $[Ca^{2+}]_i$ (i.e., both increase or both decrease), whereas a negative correlation indicates an inverse relationship between $[Ca^{2+}]_i$ and the motility parameter. A positive lag time indicates that the $[Ca^{2+}]_i$ event precedes the motility event (e.g., $[Ca^{2+}]_i$ rises before speed increases), and a negative lag time indicates that $[Ca^{2+}]_i$ follows the motility event. Table 2 summarizes the graphical interpretation of our cross-correlation analysis. The cross-correlation data were averaged over all cells at each lag time and for migration on each substrate (see Materials and Methods).

The results of the cross-correlation analysis between $[Ca^{2+}]_i$ and speed are illustrated in Fig. 7. Positive correlations are observed from 0 to +40 s, indicating that $[Ca^{2+}]_i$ peaks are associated with increases in speed, or decreases in $[Ca^{2+}]_i$ are associated with decreases in speed, with $[Ca^{2+}]_i$ changes tending to precede changes in speed by roughly 20 s. Negative correlations are observed at +60 s, and from −60 to −80 s, implying that low velocities precede calcium peaks (or that high speed precedes decreases in $[Ca^{2+}]_i$) by 60 to 80 s or follow calcium peaks by 60 s. Because $[Ca^{2+}]_i$ tends to sporadically increase from a relatively steady baseline level, we expect that cross-correlations reflect rises in $[Ca^{2+}]_i$ as opposed to drops.

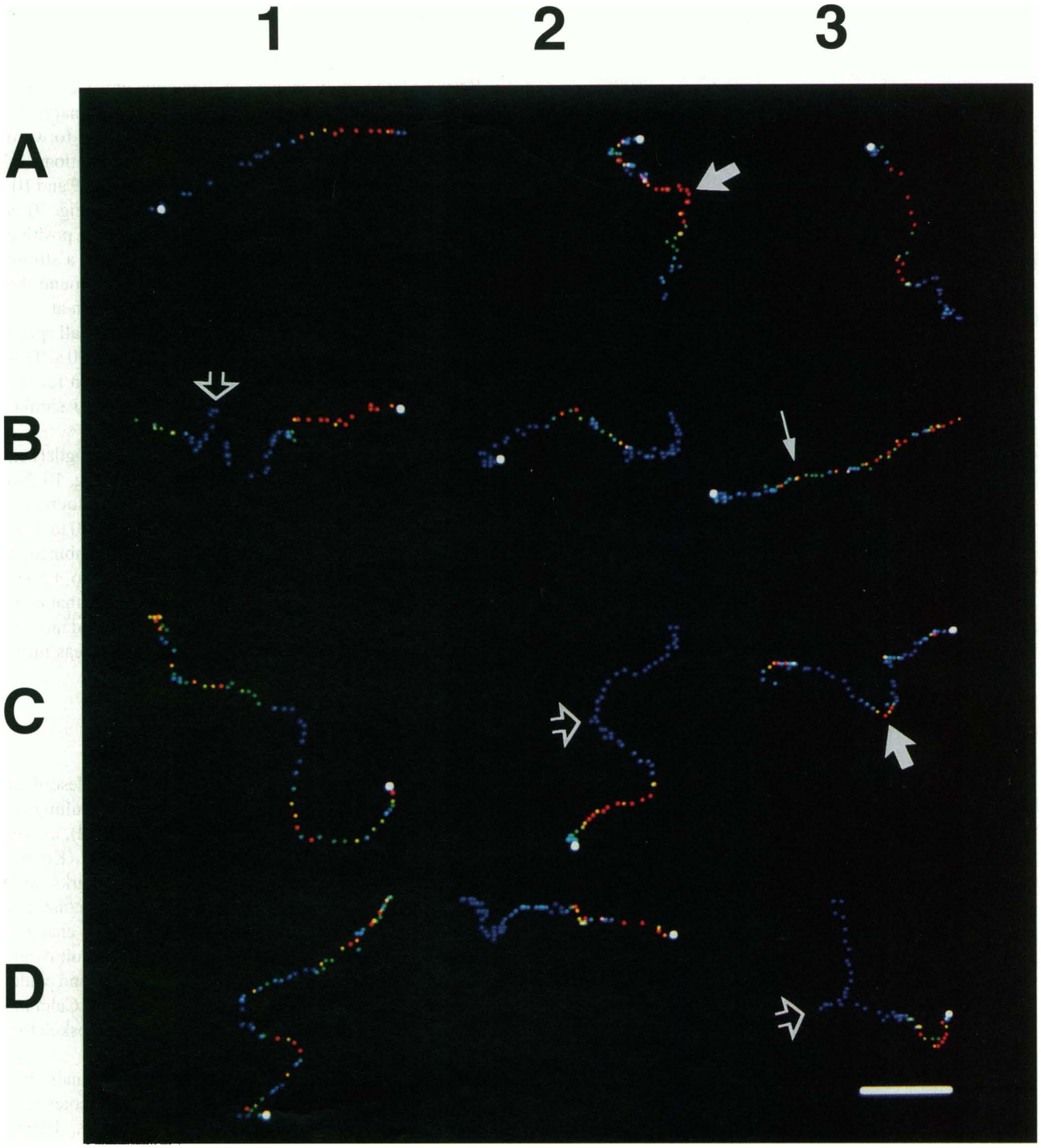

FIGURE 5 Cell tracks and occurrence of $[Ca^{2+}]_i$ spikes, illustrating heterogeneous behaviors in 12 neutrophils. Thick arrows indicate examples of turns accompanied by increases in $[Ca^{2+}]_i$. Hollow arrows are examples of turns without increases in $[Ca^{2+}]_i$. Thin arrow indicates example of calcium transients during persistent forward motion. Location of cell centroids are marked by colored symbols at 5-s intervals, with the color indicating whole cell $[Ca^{2+}]_i$ (blue indicates low $[Ca^{2+}]_i$, green intermediate, red high) determined from mean fluo-3 fluorescence (see Materials and Methods). Initial location is indicated by white symbol. Bar, 10 μm.

Cross-correlation analysis between $[Ca^{2+}]_i$ and angle change is shown in Fig. 8. A negative correlation is seen from -30 to $+60$ s when data from all substrates are combined. A positive correlation is seen at -90 s. This means that a cell is more likely to be going forward (low angle change) from $\sim$30 s before a calcium spike to $\sim$60 s after. The converse relation also will give a similar cross-correlation, in that an episode of large angle change would occur around the time

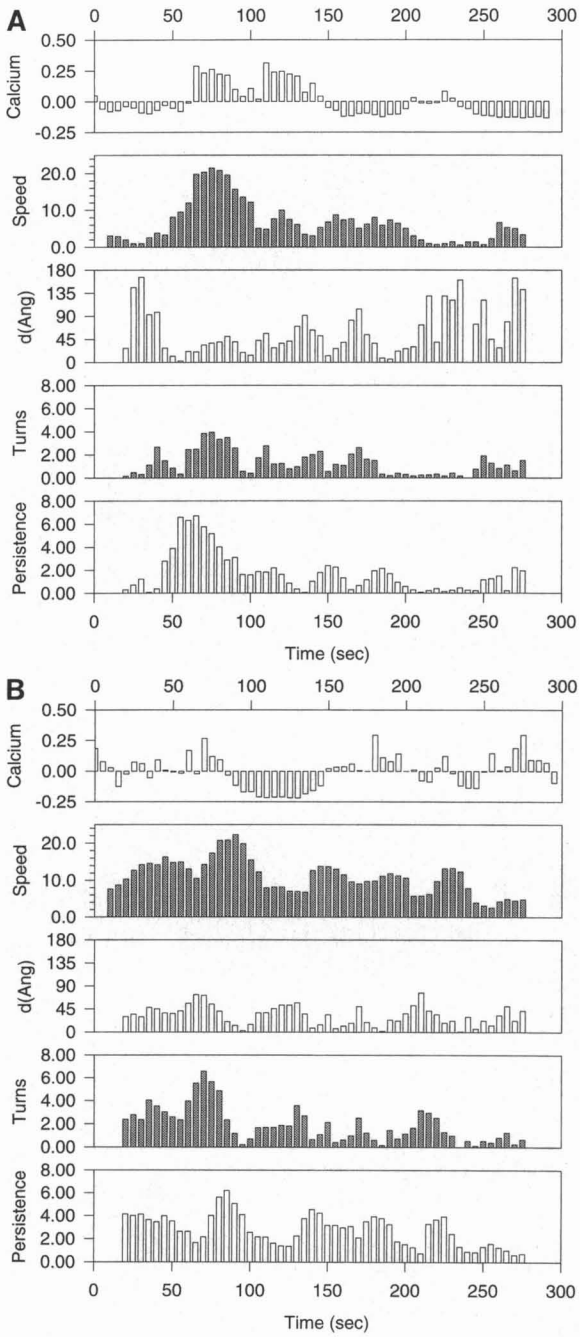

FIGURE 6 Examples of individual cell data, including normalized $[Ca^{2+}]_i$, speed, angle change, turn strength, and persistence. (*A*) Data from cell *A-3* in Fig. 5, exhibiting high correlation between $[Ca^{2+}]_i$ and speed. (*B*) Data from cell *C-1* in Fig. 5. See Materials and Methods for definitions. Calcium, $[Ca^{2+}]_i$ in arbitrary units as measured by relative fluo-3 fluorescence, normalized and mean-subtracted; speed, μm/min using 20-s time ruler; d(Ang), change in angle between incoming and outgoing vectors, in degrees; turns, turn strength, or off-axis motion; persistence, forward persistence, or on-axis motion. Time given in seconds.

of a $[Ca^{2+}]_i$ trough (i.e., a period lacking calcium spikes). Angle change was the only parameter we measured with notable substrate-dependent differences; significant negative correlations around zero were present on the highly adhesive substrates fibronectin and vitronectin, whereas no significant correlations were observed on the poorly adhesive substrate albumin.

Because large angle changes may include episodes of the cell's searching motion while it is relatively stationary, the strength of a turn was quantified by looking at the forward persistence and turn strength. The cross-correlations of $[Ca^{2+}]_i$ with these two parameters are shown in Fig. 9 and 10. The cross-correlation pattern of the persistence (Fig. 9) is similar to that for speed alone (Fig. 7), in which a positive correlation is seen from -20 to $+40$ s, indicating a strong tendency for the cell to persist in going forward around the time of a calcium spike. A negative correlation seen at -90 to -60 s implies either a large angle change or a small speed (or both) preceding a large calcium spike by 60 to 90 s. This cross-correlation pattern is opposite to the one seen for the angle-$[Ca^{2+}]_i$ cross-correlation (Fig. 8), leading to similar conclusions from both.

The cross-correlation of $[Ca^{2+}]_i$ with the turn strength (i.e., the perpendicular speed component) is shown in Fig. 10. No significant positive or negative correlations were found on any of the substrates we tested from lag times of -60 to $+60$ s. However, when data from all substrates are combined, a significant negative correlation is seen from $+40$ to $+50$ s. When taken together, our analysis of turns implies that neutrophils have a tendency to exhibit persistent forward motion around the time of a rise in total cell $[Ca^{2+}]_i$ whereas turns tend to occur during periods of low $[Ca^{2+}]_i$.

DISCUSSION

The motion of migrating neutrophils has been well described (Dunn and Zicha, 1993; Gruler, 1989; Gruler and Bultmann, 1984; Hall and Peterson, 1979; Murray et al., 1992), as has the occurrence of $[Ca^{2+}]_i$ transients in these cells (Krause et al., 1993; Marks and Maxfield, 1990a; Marks and Maxfield, 1990b). Neutrophil trajectories reveal fluctuations in speed and direction at irregular intervals, with changes occurring roughly every 60–120 s (Gruler and Bultmann, 1984). The timing of $[Ca^{2+}]_i$ spikes is also irregular and could be consistent with cyclical changes in motility. Calcium could regulate cell movement by affecting the cytoskeleton and/or adhesion to the substratum.

Although there have been many studies on signals that initiate motility (Chun and Jacobson, 1992; Devreotes and Zigmond, 1988; Jaconi et al., 1991; Kruskal et al., 1986), there have been few on cycles of signaling that would be required for continued locomotion. Neutrophils are able to migrate on low adhesion surfaces such as albumin when $[Ca^{2+}]_i$ transients are blocked (Marks et al., 1991) or even for a few minutes after their $[Ca^{2+}]_i$ has been buffered to near 0 nM (Marks et al., 1991). Therefore, there is no absolute requirement for $[Ca^{2+}]_i$ transients for motility. Observations from other cell types have suggested that $[Ca^{2+}]_i$ could be associated with cell orientation or turns (Brundage et al., 1991; Brust-Mascher et al., 1994; Gollnick et al., 1991).

TABLE 2 Interpretation of cross-correlation graphs

	Negative lag time	Positive lag time
Positive cross-correlation	High $[Ca^{2+}]_i$ follows high speed or low $[Ca^{2+}]_i$ follows low speed	High $[Ca^{2+}]_i$ precedes high speed or low $[Ca^{2+}]_i$ precedes low speed
Negative cross-correlation	High $[Ca^{2+}]_i$ follows low speed or low $[Ca^{2+}]_i$ follows high speed	High $[Ca^{2+}]_i$ precedes low speed or low $[Ca^{2+}]_i$ precedes high speed

To more rigorously examine the relationship between $[Ca^{2+}]_i$ changes and motility, we tracked a large number of neutrophils during fMLP-stimulated chemokinesis while measuring total cell $[Ca^{2+}]_i$. We studied migration on both highly adhesive (fibronectin and vitronectin) and poorly adhesive (albumin) substrates to see whether calcium-modulated adhesion might be playing a regulatory role in neutrophil migration. Changes in whole cell $[Ca^{2+}]_i$ were measured, as intracellular calcium gradients do not appear to be important in neutrophils (Marks and Maxfield, 1990a; and our preliminary data). We did cross-correlation analyses to determine the timing relationships and dependencies between the different time-dependent parameters (Dunn and Brown, 1987).

Our cross-correlation analysis revealed a positive correlation between $[Ca^{2+}]_i$ and cell speed. Significant positive correlations were seen around a lag time of zero on all substrates (negative correlations at large lag times will be discussed below). These correlations are probably due to increases in speed around the same time as increases in $[Ca^{2+}]_i$, because changes in $[Ca^{2+}]_i$ usually reflect a positive spike from a relatively flat baseline. However, the timing of the correlation was not consistent with a simple cause and effect relationship. Increases in velocity were seen before increases in $[Ca^{2+}]_i$, particularly on fibronectin, as well as after increases in $[Ca^{2+}]_i$. These results indicate a strong association between a measurable indicator of intracellular signaling and changes in cell motility but not a strict timing relationship. As the speed of migrating neutrophils is somewhat cyclical, the overall timing of increases and decreases in speed probably accounts for the negative cross-correlations we observed with speed or persistence at $\sim\pm 80$ s. It seems unlikely that events with such long lag times are directly connected mechanistically.

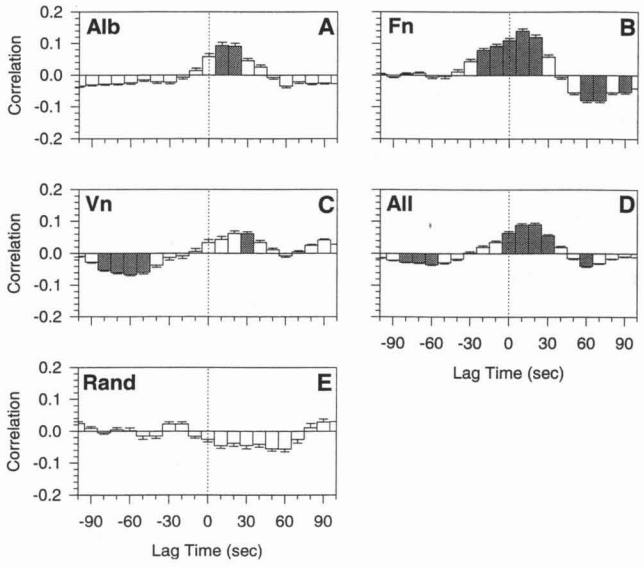

FIGURE 7 Averaged cross-correlation data of $[Ca^{2+}]_i$ versus speed on (*A*) albumin ($n = 60$); (*B*) fibronectin ($n = 61$); (*C*) vitronectin ($n = 73$); and (*D*) all substrates combined ($n = 194$). (*E*) Correlation of $[Ca^{2+}]_i$ versus speed from randomly matched cells ($n = 30$). See Materials and Methods for definitions and Table 2 for interpretation. Briefly, positive lag times indicate calcium event precedes motility event; negative lag times indicate calcium event follows motility event. Positive correlations indicate both increase (or decrease) together, negative correlations indicate one increases while the other decreases. Shaded bars indicate 95% confidence at Bonferroni significance levels ($p < 0.05$) that the mean is different from zero. Mean ± SE at each lag time.

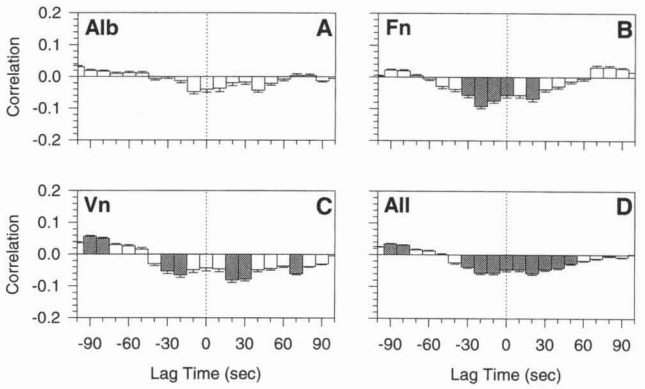

FIGURE 8 Averaged cross-correlation data of $[Ca^{2+}]_i$ versus angle change on (*A*) albumin, no significant peaks; (*B*) fibronectin; (*C*) vitronectin; and (*D*) all substrates. See Fig. 7 caption for interpretation.

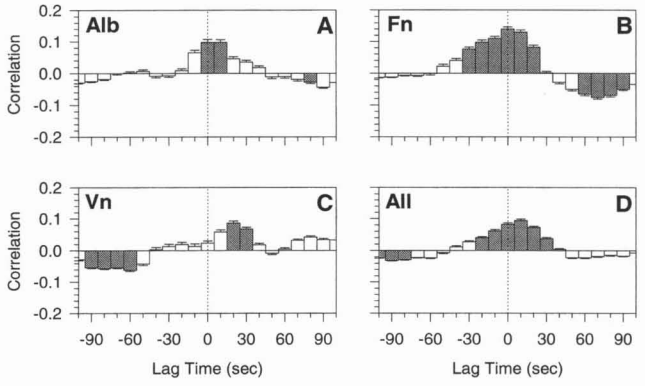

FIGURE 9 Averaged cross-correlation data of $[Ca^{2+}]_i$ versus persistence on (*A*) albumin; (*B*) fibronectin; (*C*) vitronectin; and (*D*) all substrates combined. See Fig. 7 caption for interpretation.

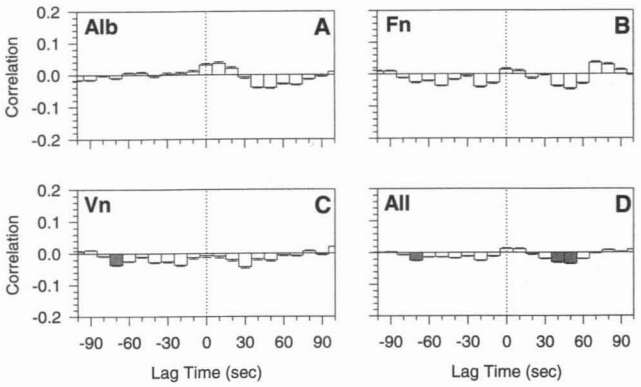

FIGURE 10 Averaged cross-correlation data of $[Ca^{2+}]_i$ versus turn strength on (*A*) albumin; (*B*) fibronectin; (*C*) vitronectin; and (*D*) all substrates. See Fig. 7 caption for interpretation.

Our cross-correlation analysis did not reveal a correlation between $[Ca^{2+}]_i$ and turns, which conflicts with data from other cell types. The choice of parameters to measure a turn is somewhat arbitrary, and our first definition was simply the change in angle. We found a significant negative correlation between angle change and $[Ca^{2+}]_i$ around a lag time of zero on all substrates. However, angle change may not be a useful parameter for measuring productive turns, because large angle changes result during periods of low speed, when the cell centroid is affected more by changes in shape than true locomotion. To account for this shortcoming, we defined a parameter we called the turn strength, which takes into account the speed of the cell. Using the turn strength, we found little correlation with $[Ca^{2+}]_i$ at any lag time. This lack of correlation is consistent with our subjective impressions from examining cell tracks (see Fig. 5).

The persistence, which is a measure of forward motion, correlated positively with $[Ca^{2+}]_i$ around a lag time of zero. Taken together with turn strength, this indicates that the increased speed observed with calcium transients is mainly in the forward direction. Our overall conclusion is that changes in $[Ca^{2+}]_i$ are not closely associated with turns in migrating neutrophils. Large numbers of cells must be examined in other cell types as well to establish whether a significant correlation between $[Ca^{2+}]_i$ and turns truly exists in those cells.

Our correlation data show that speed changes are related to intracellular signals, but they do not show that $[Ca^{2+}]_i$ is the proximal signal. Several intracellular signaling pathways are activated in migrating neutrophils (Devreotes and Zigmond, 1988), but $[Ca^{2+}]_i$ is the only one that can be directly measured in individual cells while they move. However, changes in $[Ca^{2+}]_i$, caused by release from intracellular stores (Marks and Maxfield, 1990b), are intimately linked to other signaling pathways. Hydrolysis of phosphatidylinositol bisphosphate (PIP_2) produces diacylglycerol in addition to the inositol triphosphate that is responsible for release of $[Ca^{2+}]_i$ from intracellular organelles. Stimulation of neutrophils with phorbol myristate acetate and diacylglycerols, which activate protein kinase C isoforms, leads to decreased locomotion and increased pinocytosis and surface ruffling (Keller, 1990; Roos et al., 1987). Furthermore, hydrolysis of PIP_2 can directly affect the actin cytoskeleton as PIP_2 binding modulates the ability of profilin to interact with actin (Giuliano and Taylor, 1994; Machesky and Pollard, 1993). Thus, the timing of changes in $[Ca^{2+}]_i$ can also reflect the timing of other intracellular signaling pathways that would contribute to cycles of motility.

How might calcium itself be part of an overall motility cycle? First, calcium could be acting through motor proteins such as myosin II, recently shown to colocalize with calmodulin in the contracting tails of motile fibroblasts (Gough and Taylor, 1993). Calcium-calmodulin can activate myosin light chain kinase, which in turn activates myosin II, generating contractile force and hydrostatic pressure that can propel the cell forward. Second, calcium could be acting through several other actin-binding proteins. For example, fibroblasts transfected with the calcium-regulated actin-severing and -capping protein, gelsolin, exhibited increased rates of motility (Cunningham et al., 1991). Furthermore, actin cross-linking proteins such as fodrin (Harris and Morrow, 1990) and MARCKS (Hartwig, et al., 1992) exhibit decreased cross-linking activity in the presence of high calcium. The net effect of increased $[Ca^{2+}]_i$ would hence be to favor motility by creating a low viscosity state while providing a source of actin monomers for polymerization. Third, changes in $[Ca^{2+}]_i$ could be affecting the adhesion state of the cell via surface integrins (Hendey et al., 1992). However, we found no significant substrate-dependent differences in the correlation of $[Ca^{2+}]_i$ with speed or persistence. The finding that cell speed (Fig. 7) and persistent forward motion (Fig. 9) correlate with calcium transients, that calcium-buffered cells move slower than unbuffered cells (Table 1), and that calcium-depleted cells stop moving after a few minutes (Marks and Maxfield, 1990b) all support a positive role for calcium transients in cell motility.

In summary, we have shown that high speed and persistent forward motion accompany calcium spikes in human neutrophils and that there is no relationship between turns and calcium spiking activity in these cells. Our single cell cross-correlation analysis indicates that speed peaks can occur before $[Ca^{2+}]_i$ peaks, precluding a direct causal role for $[Ca^{2+}]_i$. However, $[Ca^{2+}]_i$ clearly plays a role in modulating cell motility, as demonstrated by our calcium-buffering experiments. The overall mechanisms for coordinating all of the changes required for cycles of cell motility, including $[Ca^{2+}]_i$ and other signaling pathways, remain to be elucidated.

The authors thank Drs. Rajasekhar Ramakrishnan and Ken Dunn for their help with the statistical analysis and Moira Lawson for helpful discussions. This work was supported by National Institutes of Health grant GM34770 (F.R.M.) and Medical Scientist Training Program grant 5-T32GM07367 (J.T.H.M.) and a post-doctoral fellowship from the American Heart Association, NYC Affiliate (R.N.G.).

REFERENCES

Brundage, R. A., K. E. Fogarty, R. A. Tuft, and F. S. Fay. 1991. Calcium gradients underlying polarization and chemotaxis of eosinophils. *Science.* 254:703–706.

Brundage, R. A., K. E. Fogarty, R. A. Tuft, and F. S. Fay. 1993. Chemotaxis of newt eosinophils: calcium regulation of chemotactic response. *Am. J. Physiol.* 265:C1527–1543.

Brust-Mascher, I., R. M. Williams, and W. W. Webb. 1994. Calcium distributions in motile, electrotactic fish keratocytes measured by two-photon excited fluorescence microscopy. Presented at Biophysical Society, 38th Annual Meeting, New Orleans, LA.

Cassimeris, L., and S. H. Zigmond. 1990. Chemoattractant stimulation of polymorphonuclear leucocyte locomotion. *Semin. Cell Biol.* 1:125–134.

Caterina, M. J., and P. N. Devreotes. 1991. Molecular insights into eukaryotic chemotaxis. *FASEB J.* 5:3078–3085.

Cembrowski, G. S., J. O. Westgard, W. J. Conover, and E. C. J. Toren. 1979. Statistical analysis of method comparison data: testing normality. *Am. J. Clin. Pathol.* 72:21–26.

Chun, J. S., and B. S. Jacobson. 1992. Spreading of HeLa cells on a collagen substratum requires a second messenger formed by the lipoxygenase metabolism of arachidonic acid released by collagen receptor clustering. *Mol. Biol. Cell.* 3:481–492.

Condeelis, J., A. Bresnick, M. Demma, S. Dharmawardhane, R. Eddy, A. L. Hall, R. Sauterer, and V. Warren. 1990. Mechanisms of amoeboid chemotaxis: an evaluation of the cortical expansion model. *Dev. Genet.* 11:333–340.

Cunningham, C. C., T. P. Stossel, and D. J. Kwiatkowski. 1991. Enhanced motility in NIH 3T3 fibroblasts that overexpress gelsolin. *Science.* 251: 1233–1236.

Devreotes, P. N., and S. H. Zigmond. 1988. Chemotaxis in eukaryotic cells: a focus on leukocytes and *Dictyostelium*. *Annu. Rev. Cell Biol.* 649–686.

Dunn, G. A., and A. F. Brown. 1987. A unified approach to analysing cell motility. *J. Cell Sci. Suppl.* 8:81–102.

Dunn, G. A., and D. Zicha. 1993. Long-term chemotaxis of neutrophils in stable gradients: preliminary evidence of periodic behavior. *Blood Cells.* 19:25–41.

Eliott, S., G. H. Joss, A. Spudich, and K. L. Williams. 1993. Patterns in *Dictyostelium discoideum*: the role of myosin II in the transition from the unicellular to the multicellular phase. *J. Cell Sci.* 104:457–466.

Foskett, J. K. 1988. Simultaneous Nomarski and fluorescence imaging during video microscopy of cells. *Am. J. Physiol.* 255 (Cell Physiol. 24):C566–C571.

Fukui, Y., T. J. Lynch, H. Brzeska, and E. D. Korn. 1989. Myosin I is located at the leading edges of locomoting *Dictyostelium* amoebae. *Nature.* 341: 328–331.

Giuliano, K. A., and D. L. Taylor. 1994. Fluorescent actin analogs with a high affinity for profilin in vitro exhibit an enhanced gradient of assembly in living cells. *J. Cell Biol.* 124:971–983.

Glantz, S. A. 1992. Primer of biostatistics. McGraw-Hill, New York. 440 pp.

Gollnick, F., R. Meyer, and W. Stockem. 1991. Visualization and measurement of calcium transients in *Amoeba proteus* by fura-2 fluorescence. *Eur. J. Cell Biol.* 55:262–271.

Gough, A. H., and D. L. Taylor. 1993. Fluorescence anisotropy imaging microscopy maps calmodulin binding during cellular contraction and locomotion. *J. Cell Biol.* 121:1095–1107.

Gruler, H. 1989. Biophysics of leukocytes: neutrophil chemotaxis, characteristics and mechanisms. *In* The Neutrophil: Cellular Biochemistry and Physiology. M. B. Hallett, editor. CRC Press, Boca Raton, FL. 63–95.

Gruler, H., and B. D. Bultmann. 1984. Analysis of cell movement. *Blood Cells.* 10:61–77.

Hall, R. L., and S. C. Peterson. 1979. Trajectories of human granulocytes. *Biophys. J.* 25:365–372.

Harris, A. S., and J. S. Morrow. 1990. Calmodulin and calcium-dependent protease I coordinately regulate the interaction of fodrin with actin. *Proc. Natl. Acad. Sci. USA.* 87:3009–3013.

Hartwig, J. H., M. Thelen, A. Rosen, P. A. Janmey, A. C. Nairn, and A. Aderem. 1992. MARCKS is an actin filament crosslinking protein regulated by protein kinase C and calcium-calmodulin. *Nature.* 356:618–622.

Hendey, B., C. B. Klee, and F. R. Maxfield. 1992. Inhibition of neutrophil chemokinesis on vitronectin by inhibitors of calcineurin. *Science.* 258:296–299.

Hynes, R. O. 1992. Integrins: versatility, modulation, and signaling in cell adhesion. *Cell.* 69:11–25.

Jaconi, M. E., J. M. Theler, W. Schlegel, R. D. Appel, S. D. Wright, and P. D. Lew. 1991. Multiple elevations of cytosolic-free Ca^{2+} in human neutrophils: initiation by adherence receptors of the integrin family. *J. Cell Biol.* 112:1249–1257.

Keller, H. U. 1990. Diacylglycerols and PMA are particularly effective stimulators of fluid pinocytosis in human neutrophils. *J. Cell Physiol.* 145:465–471.

Krause, K. H., N. Demaurex, M. Jaconi, and D. P. Lew. 1993. Ion channels and receptor-mediated Ca^{2+} influx in neutrophil granulocytes. *Blood Cells.* 19:165–173.

Kruskal, B. A., S. Shak, and F. R. Maxfield. 1986. Spreading of human neutrophils is immediately preceded by a large increase in cytoplasmic free calcium. *Proc. Natl. Acad. Sci. USA.* 83:2919–2923.

Lee, J., A. Ishihara, and K. Jacobson. 1993. How do cells move along surfaces? *Trends Cell Biol.* 3:366–370.

Lilliefors, H. W. 1967. The Kolmogorov-Smirnov test for normality with mean and variance unknown. *J. Am. Stat. Assoc.* 62:399–402.

Machesky, L. M., and T. D. Pollard. 1993. Profilin as a potential mediator of membrane-cytoskeleton communication. *Trends Cell Biol.* 3:381–385.

Marks, P. W., B. Hendey, and F. R. Maxfield. 1991. Attachment to fibronectin or vitronectin makes human neutrophil migration sensitive to alterations in cytosolic free calcium concentration. *J. Cell Biol.* 112:149–158.

Marks, P. W., B. A. Kruskal, and F. R. Maxfield. 1988. Simultaneous addition of EGF prolongs the increase in cytosolic free calcium seen in response to bradykinin in NRK-49F cells. *J. Cell Physiol.* 136:519–525.

Marks, P. W., and F. R. Maxfield. 1990a. Local and global changes in cytosolic free calcium in neutrophils during chemotaxis and phagocytosis. *Cell Calcium.* 11:181–190.

Marks, P. W., and F. R. Maxfield. 1990b. Transient increases in cytosolic free calcium appear to be required for the migration of adherent human neutrophils. *J. Cell Biol.* 110:43–52.

Maxfield, F. R. 1993. Regulation of leukocyte locomotion by Ca^{2+}. *Trends Cell Biol.* 3:386–391.

Murray, J., H. Vawter-Hugart, E. Voss, and D. R. Soll. 1992. Three-dimensional motility cycle in leukocytes. *Cell Motil. Cytoskel.* 22:211–223.

Poenie, M., R. Y. Tsien, and V. A. Schmitt. 1987. Sequential activation and lethal hit measured by $[Ca^{2+}]_i$ in individual cytolytic T cells and targets. *EMBO J.* 6:2223–2232.

Press, W. H., B. P. Flannery, S. A. Teukolsky, and W. T. Vetterling. 1986. Numerical recipes: the art of scientific computing. Cambridge University Press, New York. 818 pp.

Ratan, R. R., M. L. Shelanski, and F. R. Maxfield. 1986. Transition from metaphase to anaphase is accompanied by local changes in cytoplasmic free calcium in Pt K2 kidney epithelial cells. *Proc. Natl. Acad. Sci. USA.* 83:5136–5140.

Roos, F. J., A. Zimmermann, and H. U. Keller. 1987. Effect of phorbol myristate acetate and the chemotactic peptide fNLPNTL on shape and movement of human neutrophils. *J. Cell Sci.* 88:399–406.

Scanlon, M., D. A. Williams, and F. S. Fay. 1987. A Ca^{2+}-insensitive form of fura-2 associated with polymorphonuclear leukocytes: assessment and accurate Ca^{2+} measurement. *J. Biol. Chem.* 262:6308–6312.

Schwartz, M. A. 1992. Transmembrane signalling by integrins. *Trends Cell Biol.* 2:304–308.

Sheterline, P., and J. E. Rickard. 1989. The cortical actin filament network of neutrophil leukocytes during phagocytosis and chemotaxis. *In* The Neutrophil: Cellular Biochemistry and Physiology. M. B. Hallett, editor. CRC Press, Boca Raton, FL. 141–165.

Sokal, R. R., and F. J. Rohlf. 1981. Biometry. W. H. Freeman & Co., San Francisco. 859 pp.

Theriot, J. A., and T. J. Mitchison. 1991. Actin microfilament dynamics in locomoting cells. *Nature.* 352:126–131.

Wessels, D., J. Murray, G. Jung, J. A. Hammer, and D. R. Soll. 1991. Myosin IB null mutants of *Dictyostelium* exhibit abnormalities in motility. *Cell Motil. Cytoskel.* 20:301–315.

Wessels, D., and D. R. Soll. 1990. Myosin II heavy chain null mutant of *Dictyostelium* exhibits defective intracellular particle movement. *J. Cell Biol.* 111:1137–1148.

Yamashiro, D. J., S. R. Fluss, and F. R. Maxfield. 1983. Acidification of endocytic vesicles by an ATP-dependent proton pump. *J. Cell Biol.* 97:929–934.

Zigmond, S. H., and J. G. Hirsch. 1973. Leukocyte locomotion and chemotaxis: new methods for evaluation, and demonstration of a cell-derived chemotactic factor. *J. Exp. Med.* 137:387–410.